Quantum Tunneling of Magnetization in a Metal-Organic Framework

Ying Tian, Wei Wang, Yisheng Chai, Junzhuang Cong, Shipeng Shen, Liqin Yan,
Shouguo Wang, Xiufeng Han, and Young Sun[*]

*State Key Laboratory of Magnetism and Beijing National Laboratory for Condensed Matter Physics,
Institute of Physics, Chinese Academy of Sciences, Beijing 100190, People's Republic of China*
(Received 19 July 2013; published 7 January 2014)

Resonant quantum tunneling of magnetization has been observed in a hybrid metal-organic framework where an intrinsic magnetic phase separation leads to the coexistence of long-range canted antiferromagnetic order and isolated single-ion quantum magnets. This unusual magnetic phenomenon is well interpreted based on a selective long-distance superexchange model in which the exchange interaction between transition metal ions through an organic linker depends on the position of hydrogen bonds. Our work not only extends the resonant quantum tunneling of magnetization to a new class of materials but also evokes the important role of hydrogen bonding in organic magnetism.

Metal-organic frameworks (MOFs) consisting of metal ions bridged by organic linkers have attracted a lot of recent research attention because they show an unprecedented variety of physical properties that are of great potential for many applications [1–4]. Especially, long-range magnetic and/or electric ordering can be achieved in specifically designed MOFs, which generates new types of organic magnets [5,6], ferroelectrics [7–9], and multiferroics [10–14]. Their diverse properties arise from the organic-inorganic duality that combines both merits of organic and inorganic elements within a single phase of materials. Thus, the MOFs represent a new family in condensed matter physics and provide great opportunities for the physics community [4].

On another side, the discovery of macroscopic quantum tunneling of magnetization (QTM) in nanomagnets such as ferritin [15], single-molecule [16–18], and single-ion [19–22] magnets, has stimulated remarkable research effort due to its promise for the development of quantum information and quantum computation [23]. So far, these two fields have not seen an overlap; *i.e.*, QTM has never been reported in the family of MOFs. However, in this Letter, we demonstrate for the first time that resonant QTM can be actually observed in a magnetic MOF. This is a consequence of an intrinsic magnetic phase separation in which long-range magnetic order coexists with isolated single-ion magnets that contribute to resonant tunneling of magnetization. In order to interpret such a peculiar magnetic behavior, we propose a selective long-distance superexchange model in which the superexchange interaction between transition metal ions through an organic linker depends critically on the position of hydrogen bonds.

The MOF with the ABX_3 perovskite structure investigated in this work has a formula of $[(CH_3)_2NH_2]Fe(HCOO)_3$. The crystal structure is shown in Fig. 1. The metal cations ($B = Fe^{2+}$) linked by formate groups ($X = HCOO^-$) form

the BX_3 skeleton, and the dimethylammonium (DMA) cations ($A = [(CH_3)_2NH_2]^+$) occupy the cavities. Previous studies have revealed that the DMA^+ is disordered at room temperature, but becomes cooperative ordering upon cooling due to the ordering of hydrogen bonding ($N–H \cdots O$) [24–26]. Single crystals of $[(CH_3)_2NH_2]Fe(HCOO)_3$ were prepared by solvothermal condition method. A 30 mL DMF solution containing 5 mmol metal chloride salts and 30 mL deionized water was heated in a polyphenyl-lined autoclaves for three days at 140 °C. The supernatants were transferred into a glass beaker to crystallization at room temperature, and cubic colorless crystals were obtained after three days. The crystals were filtered from the mother liquid and washed by ethanol. The powder x-ray diffraction (XRD) pattern at room temperature (Fig. S1 of [27]) confirmed the structure and phase purity of the prepared samples. The single-crystal XRD pattern suggests that the crystal is naturally grown layer by layer along the [012] direction (see Fig. S1 of [27]).
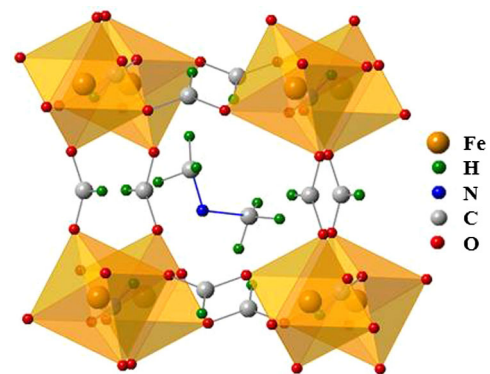

FIG. 1 (color online). The ABX_3 perovskite-like structure of $[(CH_3)_2NH_2]Fe(HCOO)_3$ with DMA^+ in the cage. The two hydrogen atoms linked with nitrogen in DMA^+ forming hydrogen bonds were not added for clarity.
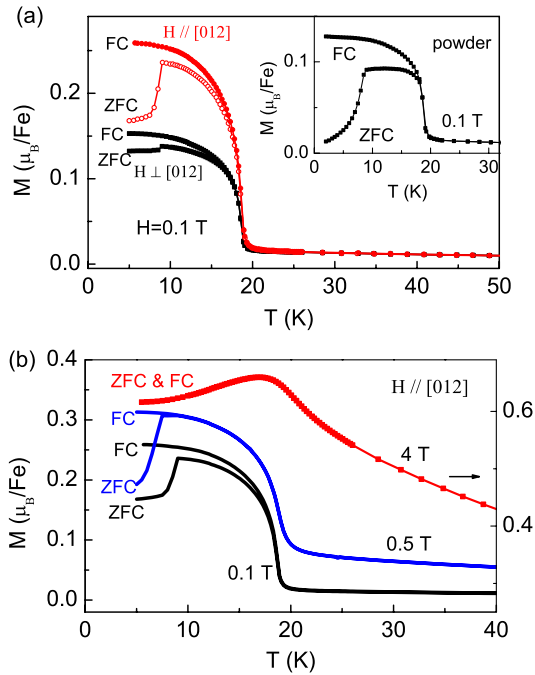
FIG. 2 (color online). (a) Magnetization as a function of temperature measured in 0. 1 T with both the ZFC and FC modes for a single crystal. Inset, magnetization as a function of temperature for a powder sample. (b) Magnetization along [012] as a function of temperature in different magnetic fields.

Figure 2(a) presents the temperature dependence of magnetization measured in 0.1 T. The MOF sample shows an apparent magnetic transition at 18.5 K. A strong magnetic anisotropy is also observed, with the easy axis along [012]. In addition to the transition at 18.5 K, there is another magnetic transition at 8.8 K, as seen in the zero-field cool (ZFC) M-T curve. The large discrepancy between the ZFC and field-cool (FC) magnetization below 8.8 K suggests a lack of pure long-range magnetic ordering. Instead, the sudden drop of the ZFC magnetization with decreasing temperature implies a blocking of magnetic moments, which is often observed in single-molecule or single-ion magnets [16,20]. Such a magnetic blocking behavior is more evident in a powder sample due to the random distribution of grain orientation, as seen in the inset of Fig. 2(a).

It is well-known that the magnetic blocking temperature depends on applied magnetic field [16]. In order to clarify whether the magnetic transition at 8.8 K is due to magnetic blocking, we measured the M-T curves with different magnetic fields. As seen in Fig. 2(b), the sudden drop of the ZFC magnetization shifts to lower temperature with increasing magnetic field, consistent with the blocking behavior [16]. In a high enough magnetic field ($H = 4$ T), the blocking behavior disappears and the ZFC and FC magnetization is identical because all the blocked magnetic moments are magnetized to saturation. The decay of magnetization with decreasing temperature measured in

4 T indicates a antiferromagneticlike order below 18.5 K. In order to further clarify the nature of the magnetic transition at 18.5 K, we performed additional experiments (Figs. S2 and S3 of [27]). The results support a paramagnetic to spin canted antiferromagnetic (CAFM) transition. This is consistent with previous reports of weak ferromagnetism due to CAFM in the isostructural MOFs containing Co or Ni [28]. The two consecutive magnetic transitions strongly indicate that there could be two coexisting magnetic components at low temperature.

The coexistence of two magnetic phases in the MOF is further confirmed by the isothermal magnetization. Figure 3(a) shows the M-H curve along [012] at 2 K. A linear dependence is seen in high magnetic field range and an apparent hysteresis is observed in the low-field range. The linear dependence of magnetization without any hysteresis is typical for long-range antiferromagnetic ordering. After subtracting the linear dependence, we then obtain the M-H hysteresis loop at 2 K shown in Fig. 3(b). The stair-shaped hysteresis loop at low temperature is a strong characteristic of resonant QTM, which has been generally observed in single-molecule and single-ion quantum magnets [16–23].

Another strong evidence for the existence of single-ion quantum magnets in the MOF comes from the ac magnetic susceptibility. As shown in Fig. 3(c), the out of phase of ac magnetic susceptibility (χ'') along [012] shows a pronounced frequency-dependent maximum in addition to the sharp transition at 18.5 K. The plot of the maximum position VS time (or frequency) shown in Fig. 3(d) follows an Arrhenius relation: $\tau = \tau_0 \exp(\Delta E/\kappa_B T)$, which is another characteristic of single-ion quantum magnets [19–22]. The linear fitting to the Arrhenius relation resulted
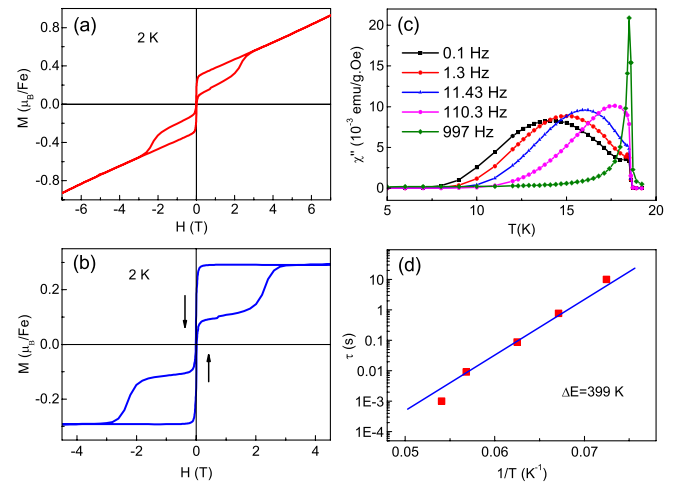

FIG. 3 (color online). (a) The M-H loop along [012] at 2 K. (b) The stair-shaped hysteresis loop obtained by subtracting the linear dependence is a sign of resonant QTM. (c) The out-of-phase of ac magnetic susceptibility along [012] at various frequencies as a function of temperature. (d) Arrhenius analysis of the magnetic relaxation process of single-ion magnets.

in a relaxation time of $\tau_0 = 1.8 \times 10^{-12}$ s and an energy barrier of $\Delta E = 399$ K. This energy barrier is much higher than those of cluster-based single-molecular magnets, but is comparable to that in certain single-ion magnets [20]. Therefore, all the above magnetic features support the coexistence of two distinctive magnetic components in the MOF, one with the long-range CAFM order and the other showing characteristics of single-ion quantum magnets.

The coexistence of both long-range magnetic order and individual single-ion quantum magnets in the MOF is striking because a long-range magnetic order requires strong exchange coupling between neighboring magnetic moments, whereas single-ion magnets mean isolated magnetic ions with negligible exchange interactions. To understand this peculiar magnetic behavior, we need to first comprehend the origin of the exchange interactions in the MOF. When the transition-metal cations M are separated by main group ligand atoms L, direct exchange between the d orbitals of M is very unlikely. Instead, exchange may take place by taking into account hopping via the intermediate p orbital of L anions. This indirect exchange mechanism through M-L-M path is called superexchange (SE) and has become well-known since 1960s [29]. In the early of this century, exchange involving double ligand atoms through M-L-L-M path, termed as super-superexchange (SSE) interaction was discussed in details by chemists [30,31]. Here, in the studied MOFs, the transition metal cations are separated by a formate group involving at least three atoms (O-C-O). This form of superexchange through multiple atoms (M-L-L-L-M) may be called a long-distance superexchange (LDSE).

In general, exchange interactions between localized magnetic moments can be described by the Heisenberg model [32]

$$H = -J S_1 \cdot S_2, \qquad (1)$$

$$J \approx -\frac{4t^2}{U_{\text{eff}}}, \qquad (2)$$

where J is the exchange energy, t is the hopping integral, and U_{eff} is the effective on site repulsion. In the case of conventional SE interaction (M-L-M), the strength of J strongly depends on the geometry of exchange path that determines the hopping integral t, and can be estimated by the Goodenough-Kanamori rules [29] on the basis of the bond angle, the symmetry properties of the d orbitals containing unpaired spins, and the number of unpaired spins at M. In addition to that, the relative strength of SSE interaction (M-L-L-M) was found to depend largely on the overlap between the two p orbitals residing on L [30,31]. Similarly, the LDSE in the studied MOFs must have a critical dependence on the geometry of exchange path (M-L-L-L-M).
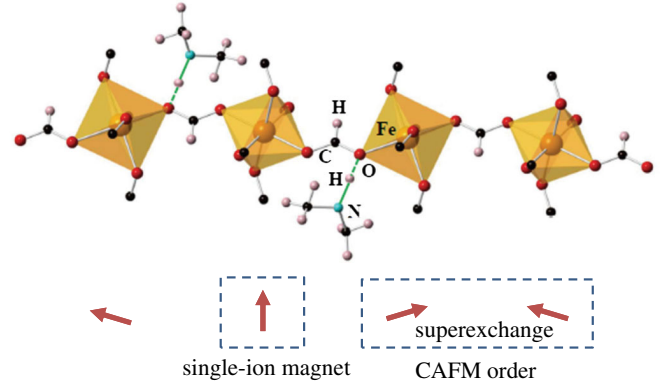

FIG. 4 (color online). Scheme of magnetic phase separation in the MOF. The superexchange interaction between Fe^{2+} through the formate group leads to the CAFM order. In contrast, the superexchange interaction is broken when the formate group is coupled with a DMA^+ via the hydrogen bonding. The isolated Fe^{2+} ions without superexchange behave as single-ion quantum magnets.

As illustrated in Fig. 4, the transition metal cations (Fe^{2+}) are bridged by organic linkers to form the framework. Depending on the position of the DMA^+ cation in the cavity, there are two types of linker: one is a pure formate group and another is a formate group coupled with the DMA^+ cation via a hydrogen bond ($N - H \cdots O$). The Fe^{2+} cations linked by a pure formate group can form a CAFM order via the LDSE interaction through Fe-O-C-O-Fe exchange path. In contrast, when a hydrogen bond is coupled with the formate group, the geometry of the exchange path could be altered significantly. Firstly, the hydrogen bond usually causes a shift of an O atom toward the DMA^+ cation, resulting in a bending of exchange path. According to the Goodenough-Kanamori rules [29], the strength of the SE interaction decreases as the bond angle becomes smaller. Secondly, the attractive potential produced by the hydrogen bond could induce a rotation of p orbitals of O, which could reduce the overlap between p orbitals of O and d orbitals of Fe^{2+} as well as that between two p orbitals in the middle of the path. Therefore, the LDSE interaction in the MOF could be significantly suppressed by hydrogen bonds.

Considering the ratio of $A:X = 1:3$ in the ABX_3 perovskite and the fact that each A cation (DMA^+) provides two hydrogen bonds, only $1/3$ formate groups are free of hydrogen bonds. It has been confirmed that the nitrogen atom of DMA^+, and consequently the hydrogen bonds, tends to be ordered at low temperature [24–26]. If the hydrogen bonds are completely ordered, a long-range magnetic order could be formed throughout the MOF. In reality, there could be a certain amount of Fe^{2+} that are surrounded by hydrogen-bond coupled linkers due to the partial disorder of hydrogen bonds. As $Fe^{2+}(3d^6)$ in octahedral coordination of the perovskite structure has a relatively strong uniaxial magnetic anisotropy [33], those

isolated Fe^{2+} ions without LDSE interaction would behavior as individual single-ion quantum magnets. Therefore, the coexistence of both long-range magnetic order and single-ion quantum magnets in the MOF is a natural consequence of the ordered and disordered distribution of hydrogen bonds that determine whether the LDSE through an organic linker could happen.

In summary, our experiments in a magnetic MOF with a perovskitelike structure have demonstrated an intrinsic magnetic phase separation in which long-range magnetic order coexists with individual single-ion magnets showing resonant QTM. This peculiar magnetic behavior is well interpreted in terms of the influence of hydrogen bonding on the LDSE interaction between transition metal ions through an organic linker. Since the LDSE interaction is sensitive to the geometry of exchange path, a hydrogen bond coupled on the organic linker could effectively alter the geometry of exchange path and break the LDSE interaction. In this way, the magnetic structure depends on the position of hydrogen bonds.

*Corresponding author.
youngsun@iphy.ac.cn

[1] A. K. Cheetham and C. N. R. Rao, Science **318**, 58 (2007).
[2] S. Kitagawa, R. Kitaura, and S. Noro, Angew. Chem., Int. Ed. Engl. **43**, 2334 (2004).
[3] O. M. Yaghi, G. M. Li, and H. L. Li, Nature (London) **378**, 703 (1995).
[4] C. N. R. Rao, A. K. Cheetham, and A. Thirumurugan, J. Phys. Condens. Matter **20**, 083202 (2008).
[5] K. L. Hu, M. Kurmoo, Z. Wang, and S. Gao, Chem. Eur. J. **15**, 12050 (2009).
[6] D. F. Weng, Z. M. Wang, and S. Gao, Chem. Soc. Rev. **40**, 3157 (2011).
[7] P. Jain, N. S. Dalal, B. H. Toby, H. W. Kroto, and A. K. Cheetham, J. Am. Chem. Soc. **130**, 10450 (2008).
[8] W. Zhang and R.-G. Xiong, Chem. Rev. **112**, 1163 (2012).
[9] A. Stroppa, P. Barone, P. Jain, J. M. Perez-Mato, and S. Picozzi, Adv. Mater. **25**, 2284 (2013).
[10] P. Jain, V. Ramachandran, R. J. Clark, H. D. Zhou, B. H. Toby, N. S. Dalal, H. W. Kroto, and A. K. Cheetham, J. Am. Chem. Soc. **131**, 13625 (2009).
[11] G. C. Xu, W. Zhang, X. M. Ma, Y. H. Chen, L. Zhang, H. L. Cai, Z. M. Wang, R. G. Xiong, and S. Gao, J. Am. Chem. Soc. **133**, 14948 (2011).
[12] B. Kundys, A. Lappas, M. Viret, V. Kapustianyk, V. Rudyk, S. Semak, C. Simon, and I. Bakaimi, Phys. Rev. B **81**, 224434 (2010).
[13] A. Stroppa, P. Jain, P. Barone, M. Marsman, J. M. Perez-Mato, A. K. Cheetham, H. W. Kroto, and S. Picozzi, Angew. Chem., Int. Ed. Engl. **50**, 5847 (2011).
[14] W. Wang, L.-Q. Yan, J.-Z. Cong, Y.-L. Zhao, F. Wang, S.-P. Shen, T. Zou, D. Zhang, S.-G. Wang, X.-F. Han, and Y. Sun, Sci. Rep. **3**, 2024 (2013).
[15] D. D. Awschalom, D. P. DiVincenzo, and J. F. Smyth, Science **258**, 414 (1992).
[16] J. R. Friedman, M. P. Sarachik, J. Tejada, and R. Ziolo, Phys. Rev. Lett. **76**, 3830 (1996).
[17] L. Thomas, F. Lionti, R. Ballou, D. Gatteschi, R. Sessoli, and B. Barbara, Nature (London) **383**, 145 (1996).
[18] B. Barbara, L. Thomas, F. Lionti, I. Chiorescu, and A. Sulpice, J. Magn. Magn. Mater. **200**, 167 (1999).
[19] S. D. Jiang, B. W. Wang, G. Su, Z. M. Wang, and S. Gao, Angew. Chem., Int. Ed. Engl. **49**, 7448 (2010).
[20] S. D. Jiang, B. W. Wang, H. L. Sun, Z. M. Wang, and S. Gao, J. Am. Chem. Soc. **133**, 4730 (2011).
[21] S. Mossin, B. L. Tran, D. Adhikari, M. Pink, F. W. Heinemann, J. Sutter, R. K. Szilagyi, K. Meyer, and D. J. Mindiola, J. Am. Chem. Soc. **134**, 13651 (2012).
[22] S. D. Jiang, S. S. Liu, L. N. Zhou, B. W. Wang, Z. M. Wang, and S. Gao, Inorg. Chem. **51**, 3079 (2012).
[23] J. R. Friedman and M. P. Sarachik, Annu. Rev. Condens. Matter Phys. **1**, 109 (2010).
[24] T. Besara, P. Jain, N. S. Dalal, P. L. Kuhns, A. P. Reyes, H. W. Kroto, and A. K. Cheetham, Proc. Natl. Acad. Sci. U.S.A. **108**, 6828 (2011).
[25] D. W. Fu, W. Zhang, H. L. Cai, Y. Zhang, J. Z. Ge, R. G. Xiong, S. D. Huang, and T. Nakamura, Angew. Chem., Int. Ed. Engl. **50**, 11947 (2011).
[26] M. Sánchez-Andújar, S. Presedo, S. Yáñnez-Vilar, S. Castro-García, J. Shamir, and M. A. Señarís-Rodríguez, Inorg. Chem. **49**, 1510 (2010).
[27] See Supplemental Materials at http://link.aps.org/supplemental/10.1103/PhysRevLett.112.017202 for the x-ray diffraction patterns, M-T and M-H curves.
[28] X.-Y. Wang, L. Gan, S.-W. Zhang, and Song Gao, Inorg. Chem. **43**, 4615 (2004).
[29] J. B. Goodenough, *Magnetism and the Chemical Bond* (John Wiley & Sons, New York, London, 1963).
[30] M.-H. Whangbo, H.-J. Koo, D. Dai, and D. Jung, Inorg. Chem. **42**, 3898 (2003).
[31] M.-H. Whangbo, H.-J. Koo, and D. Dai, J. Solid State Chem. **176**, 417 (2003).
[32] R. Skomski, *Simple Models of Magnetism* (Oxford University Press, New York, 2008).
[33] G. F. Dionne, *Magnetic Oxides* (Springer, New York, 2009).